

Eastern Kentucky University

Encompass

Honors Theses

Student Scholarship

Spring 2023

Application of Electrical Resistivity Tomography (ERT) to Wetland Hydrogeology: An Assessment of the Efficacy of Array Configurations

Wynter Monjarez
alayah_berg1@mymail.eku.edu

Follow this and additional works at: https://encompass.eku.edu/honors_theses

Recommended Citation

Monjarez, Wynter, "Application of Electrical Resistivity Tomography (ERT) to Wetland Hydrogeology: An Assessment of the Efficacy of Array Configurations" (2023). *Honors Theses*. 973.
https://encompass.eku.edu/honors_theses/973

This Open Access Thesis is brought to you for free and open access by the Student Scholarship at Encompass. It has been accepted for inclusion in Honors Theses by an authorized administrator of Encompass. For more information, please contact Linda.Sizemore@eku.edu.

EASTERN KENTUCKY UNIVERSITY

Application of Electrical Resistivity Tomography (ERT) to Wetland Hydrogeology: An
Assessment of the Efficacy of Array Configurations

Honors Thesis
Submitted
in Partial Fulfillment
of the
Requirements of HON 420
Spring 2023

By
Aliyah Wynter Monjarez

Mentor
Dr. John White, Professor
Department of Physics, Geosciences, and Astronomy

Application of Electrical Resistivity Tomography (ERT) to Wetland Hydrogeology: An
Assessment of the Efficacy of Array Configurations

Aliyah Wynter Monjarez

Dr. John White, Department of Physics, Geosciences, and Astronomy

Abstract — Electrical Resistivity Tomography (ERT) is a geophysical technique used to measure and map the resistivity of the subsurface. Resistivity (expressed in units of Ohm-meters), the inverse of conductivity, is an intrinsic property of earth materials that is a function of their material composition, void space, and water content. ERT is frequently used for mineral and groundwater exploration, but this technique can be used for any study that requires information of the near-surface environment. Resistivity is determined by applying a known direct current on one electrode pair (labeled C1 and C2) and taking measurements of the voltage potential on another electrode pair (labeled P1 and P2), which is used to create a modeled pseudosection from the data collected. The two most commonly used electrode array configurations are Schlumberger and Dipole-Dipole. In this study, we test the efficacy of various array configurations to determine which one is best suited to help us understand the hydrogeology of geographically isolated wetlands (GIWs). GIWs are ecologically significant systems that provide numerous benefits to the surrounding area such as water storage, water quality improvement, sediment and carbon retention, and flood protection, to name a few. Using twenty-eight electrodes with varying spacing, we were able to conduct these two array configurations on the 977N (natural) wetland in the Daniel Boone National Forest, as well as on an oxbow bend in Taylor Fork Ecological Area. Our models suggest that the Schlumberger array provides

the most accurate results. Results from the dipole-dipole array are noisy and provide a chaotic image of the subsurface whereas the Schlumberger modeled pseudosection strongly agrees with existing core data.

Keywords and Phrases — Electrical Resistivity Tomography, Wetlands, Hydrology, Vertical Electrical Sounding

Table of Contents

Title.....	i
Abstract.....	ii
Keywords and Phrases.....	iii
List of Figures.....	v
Acknowledgements.....	vi
Introduction.....	1
Objectives.....	2
Materials and Methods.....	6
Field Sites.....	8
Data Acquisition and Processing.....	11
Results and Discussion.....	22
Conclusion.....	24
Appendix One.....	25
References.....	30

List of Figures

Figure 1. Average Loss of Wetlands Globally.....	3
Figure 2. VES Method Diagram.....	5
Figure 3. AGI Inc. SuperSting R1.....	7
Figure 4. Aerial view of the 977N Field Site.....	9
Figure 5. Aerial view of the Taylor Fork Field Site	9
Figure 6. Average Annual Precipitation in Kentucky.....	10
Figure 7. Core Data Diagram.....	12
Figure 8. 977N Dipole-Dipole Pseudosection.....	13
Figure 9. 977N Schlumberger Pseudosection.....	14
Figure 10. 977N Dipole-Dipole/Schlumberger Merge Pseudosection.....	15
Figure 11. Taylor Fork Dipole-Dipole Pseudosection One.....	16
Figure 12. Taylor Fork Dipole-Dipole Pseudosection Two.....	17
Figure 13. Taylor Fork Schlumberger Pseudosection One.....	18
Figure 14. Taylor Fork Schlumberger Pseudosection Two.....	19
Figure 15. Taylor Fork Wenner-Schlumberger Pseudosection One.....	20
Figure 16. Taylor Fork Wenner-Schlumberger Pseudosection Two.....	21
Figure 17. Three Most Common Array Configurations.....	23
Figure 18. Necessary Field ERT Equipment.....	26
Figure 19. Proper Electrode Connections.....	28

Acknowledgements

I would like to thank Dr. John White for his guidance throughout this endeavor and unwavering support. With Dr. White's aid, I truly feel like a geoscientist. I thank the ECU Honors College for giving me the opportunity to complete this thesis project. Additional thanks to Dr. Kelly Watson and Dr. David Brown for aiding in this project's development. A special thank you to the National Science Foundation's Research for Undergraduates Program and Eastern Kentucky University for the initial funding for this project. A final thanks you to my REU peers for advice and support as well as the Physics, Geosciences, and Astronomy department staff and students. Without the aid of the aforementioned people, this project would not have made it off the ground. Thank you.

Introduction

Wetlands are transitional environments characterized by constantly changing water levels. “A wetland is an ecosystem that depends on constant or recurrent, shallow inundation or saturation at or near the surface of the substrate. The minimum essential characteristics of a wetland are recurrent, sustained inundation or saturation at or near the surface and the presence of physical, chemical, and biological features reflective of the recurrent, sustained inundation or saturation” (National Research Council, 1995). This paper is predominantly focused on a specific kind of wetland referred to as a geographically isolated wetland (GIW). GIWs are areas in which there is no obvious connection to surrounding bodies of water or streams, meaning that they are surrounded by otherwise undersaturated lands (Tiner et al., 2002). It is important to understand that these GIWs are only isolated in a geographical sense, and does not imply that they are completely isolated. GIWs may or may not be interconnected to the groundwater system or to one another underneath the subsurface (Tiner, 2003). For the purpose of this paper, we will define GIWs as areas surrounded by uplands, with no obvious surface connection.

GIWs are formed in topographic depressions. These depressions are inundated during periods of high precipitation. When the precipitation in these areas exceeds the drainage capacity of the near surface soils, the wetlands accumulate surface water. Generally, this accumulation of water is limited to just a few centimeters in depth (Rosa et al., 2022). When a wetland is inundated, the accumulation of water can be permanent, but is more than likely going to be temporary. Wetlands are cyclical in nature, meaning they drain and refill throughout the course of a year. This is influenced not only by the

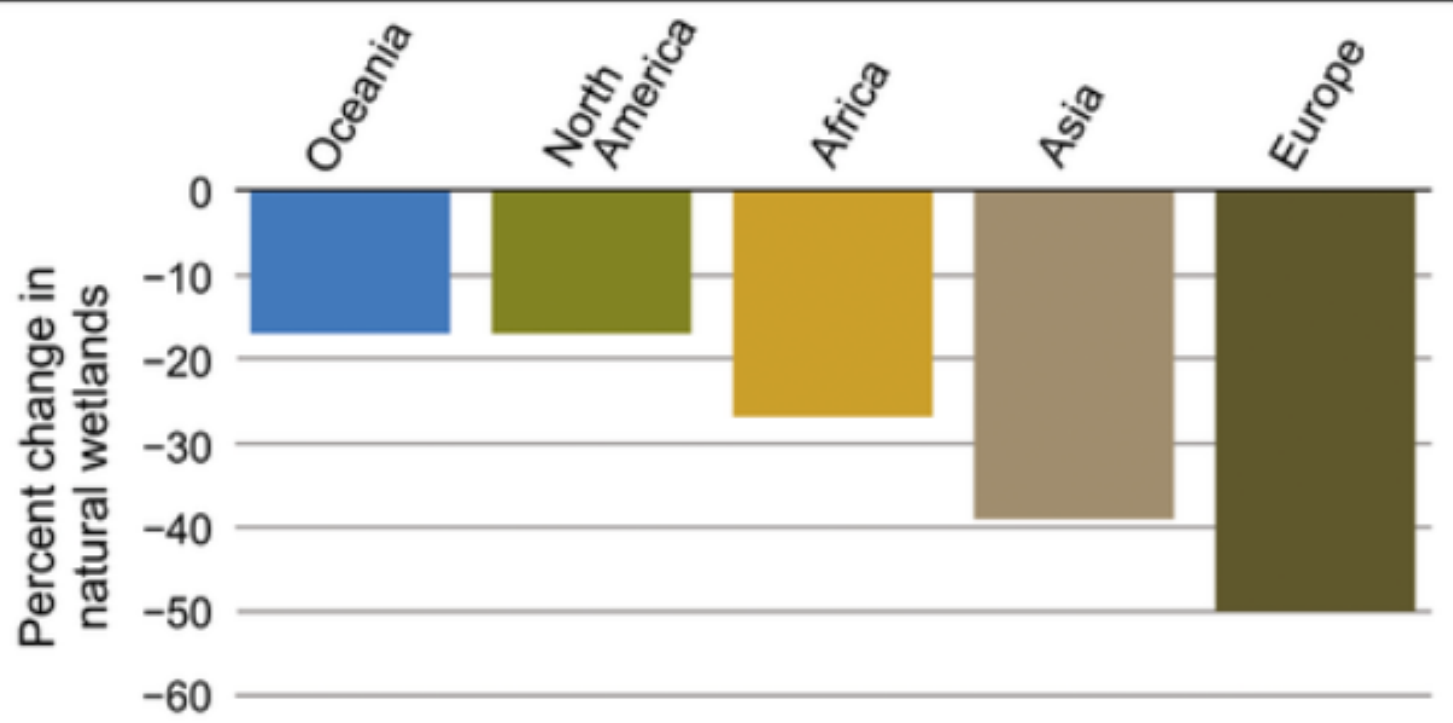
topography of an area, but also by the climate. A particularly wet season can result in longer periods of water retention, while a dry season can result in a longer period of drainage (Rosa et al., 2022).

The soils that allow for this accumulation of surface water are called hydric soils. These soils are saturated for long periods of time, enough to make them anaerobic, or without excess oxygen (Beall, 2020). Wetlands have two kinds of hydric soils, organic and mineral. Mineral wetland soils contain less than 20% organic material while organic wetland soils, also called peat, contain more than 20% organic material. Organic soil is formed over time as material decays in a saturated, anaerobic environment (Koch, 2022).

GIWs, whether composed of organic or mineral soils, are incredibly important features of any landscape. They improve water quality and carbon retention, as well as provide flood protection, biodiverse habitats, pesticide protection, and more. These systems are paramount to the continuation of these environmental services (Golden et al., 2017; Koch, 2022; Rosa et al., 2022).

Objectives

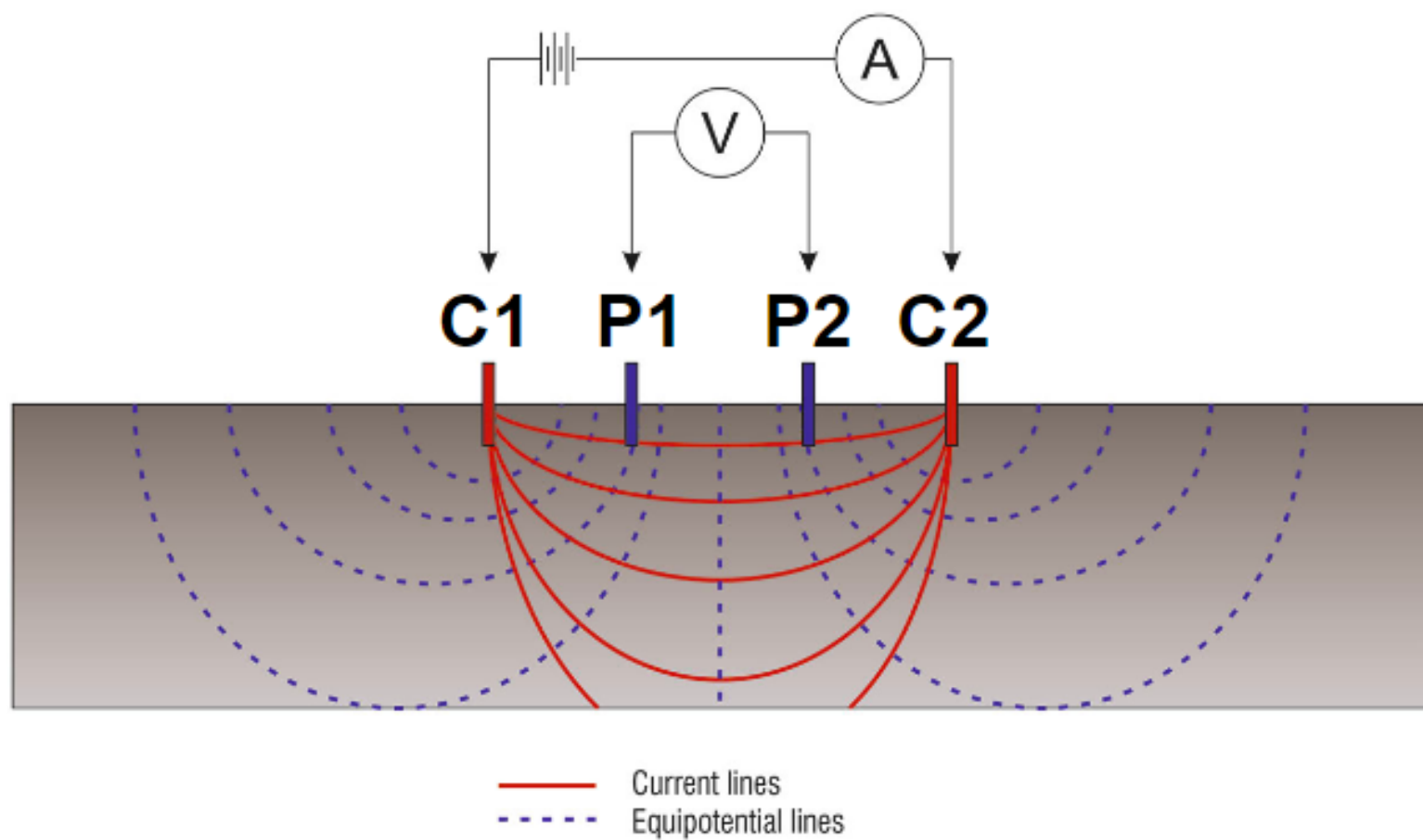
Despite all the benefits wetlands provide, they are often left unprotected (*Figure 1*). There is a lack of policy in many places to protect these areas, particularly GIWs. Due to their variability, there is an absence of a holistic definition and understanding of wetlands (Golden et al., 2017; Rosa et al., 2022). To protect these areas and to change policy, it is imperative that these areas are examined, and that current research is presented and modeled to policy makers and the general public (Golden et al., 2017; Dixon et al., 2016).



The incorporation of physical models in studies of GIWs is critical to develop protection plans for these areas. Currently, investigation techniques involve well monitoring, hydraulic conductivity measurements, auger boring, and other various geophysical processes. These techniques are commonly used due to their accuracy when analyzing hydrologic dynamics. However, establishing a well in these small, delicate systems may harm the natural hydrodynamics of the system. Well monitoring is also time consuming and resource intensive. Thus, it is not a practical method especially in the D.B.N.F. where there are abundant GIWs (Rosa et al., 2022).

Electrical resistivity tomography (ERT), is a geophysical technique that has historically been used for resource exploration. More recently, this method has been utilized for all kinds of hydrological research and environmental monitoring (Okopokhi and White, 2019; Moskal et al., 2020; Moreira et al., 2021; Yopp et al., 2021). Thus, we have applied this technique to model these GIWs to improve our understanding of them.

ERT is a near-surface geophysical method that provides a two-dimensional (2D) image of the near subsurface. This resultant image is called a pseudosection — an image of modeled resistivity values that approximate a geological cross-section of the subsurface. One popular method is vertical electrical sounding (VES). VES (sometimes referred to as electrical drilling) is used in both the Wenner and Schlumberger array configurations. VES is widely considered the original method for this technique (*Figure 2*). This visualization provides an important perspective when understanding the process of wetlands and eventually their interconnectivity (Rosa et al., 2022; Everest Geophysics, 2019).



When using ERT, it is imperative that one chooses the best array configuration for the research site as well as the data one wants to collect. The array configuration refers to the spacing between each electrode, as well as the electrical paths of the electrodes. The final measurements are determined by the spacing between electrodes. Longer spacings provide deeper subsurface measurements while shorter spacing provides shallower, more detailed measurements. The depth of the resultant data is ~20% of the survey length. However, deeper surveys suffer a reduction in resolution. Thus, the importance of choosing the correct array for the site is crucial to representing the actual subsurface geology. Using a suboptimal array configuration could result in inaccurate models (Rosa et al., 2022).

Materials and Methods

The instrumentation used for our ERT research is the SuperSting R1 (*Figure 3*). The SuperSting R1 is an electrical resistivity meter produced by Advanced Geosciences, Inc. (AGI) (AGIUSA, 2022d). This machine allows us to measure the flow of electricity in the subsurface through the use of probes placed in regular spacing. Additionally, it regulates the input current, sends instructions to the switchbox re: the array configuration, and records the voltage on the potential electrodes (Reed, 2022). The measured values provide apparent resistivity values in Ohm-meters, which can then be used to create pseudosections from inverse modeling. For our research, we utilized twenty-eight electrodes, the maximum allowable with the SuperSting R1.

Additionally, we used the AGI SuperSting R1 Adapter Box as a means to ensure our SuperSting R1 was calibrated properly (AGIUSA, 2022c). Before each field day, we ran the SuperSting through two processes. First, a receiver test, and then a contact



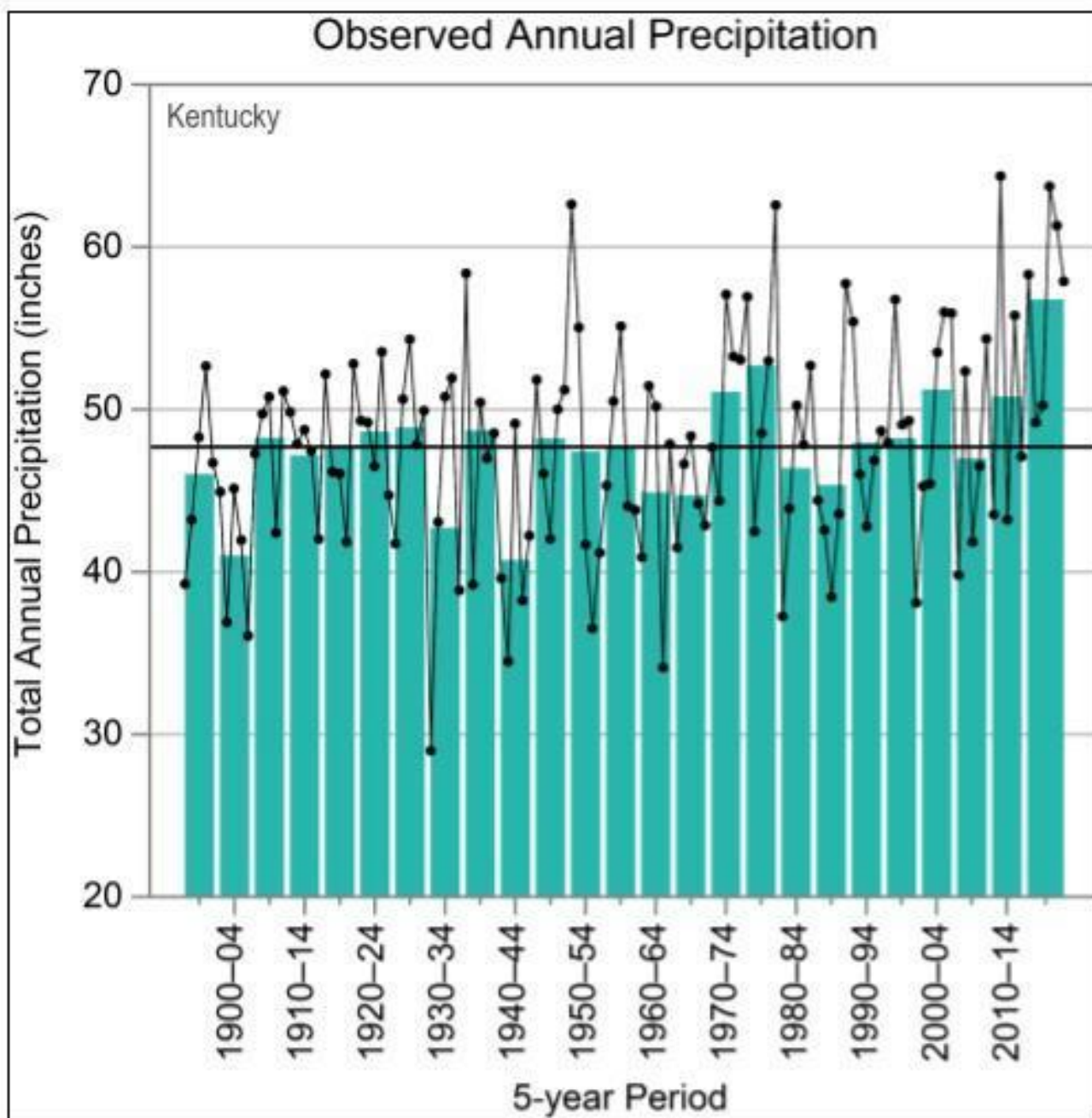
resistance test. The contact resistance test allows us to confirm that all the electrodes are connected to the wire properly and that there is good contact to the ground surface. We looked for values less than $1.8 \text{ Ka}\Omega$ (AGIUSA, 2022b). Additional equipment includes a generator to power the machines, measuring tapes, gloves, flagging, rubber mallet, connecting wires, etc. The operating procedures are detailed in appendix one (adapted from Moskal et al., 2021).

Field Sites

This study was conducted using two primary field locations: the Daniel Boone National Forest (D.B.N.F.) in Morehead, KY (*Figure 4*) and Taylor Fork Ecological Area in Richmond, KY (*Figure 5*). The coordinates for these sites were $38^{\circ}14'25.13''\text{N}$, $83^{\circ}23'53.99''\text{W}$ and $37^{\circ}42'58.78''\text{N}$, $84^{\circ}17'44.89''\text{W}$ respectively. In the D.B.N.F. site, we conducted tests on the 977N (977 Natural) wetland. In the Taylor Fork site, we conducted tests on an oxbow bend. Both sites had highly saturated surface soils.

Kentucky is classified as a humid subtropical climate (Cfa) according to the Köppen-Geiger classification. In this scheme, “C” denotes a “temperate climate” with average temperatures between 0° and 18°C in the coldest month, “f” denotes significant precipitation in all seasons with no distinct dry season, and “a” denotes hot summers with an average temperature $>22^{\circ}\text{C}$ in the warmest month (Climate Data, 2022). In general, the state has a “warm temperate climate” with has hot, humid summers and cold, rainy winters. During the year, Kentucky has an average rainfall of $\sim 147 \text{ cm}$ (*Figure 6*). The bulk of this precipitation occurs in the spring and summer (Kunkel, 2022). Our research was conducted in late June through early September. This was the ideal time of year for field tests as ERT requires relatively saturated soils.





Both areas of study are protected natural areas. There is little construction or human interference in these areas. While the Taylor Fork site location has minimal trail construction, we do not believe it has impacted the data collected. The 977N wetland remains untouched by construction but does contain human-made wells. Again, we do not believe these have impacted the collected data. However, we did use the core data from these wells when verifying our results (*Figure 7*) (Yopp et al., 2021).

Data Acquisition and Processing

After running consecutive scans at the 977N wetland as well as the Taylor Fork oxbow bend, we used the raw data and the AGI 2D EarthImager software to model pseudosections. AGI 2D EarthImager is a software system that models inversion (apparent resistivity) and induced polarization. With the data collected in the field by the SuperSting R1, we were able to develop our models in this system (AGIUSA, 2022a). We also georeferenced each scan by creating a terrain file that describes the relative position of each electrode with respect to both distance and elevation. This ensured the final models accounted for elevation change. Pictured are the results of each scan (*Figures 8-16*). Processing procedures are detailed in appendix one (Moskal et al., 2021).

All scans required removal of noisy data points. When removing noisy data points, our goal was to remove less than 5% of the data at a time in sequence until the RMS error was ideally below 5%. Some figures required much more data removal than others. The warm tones denote high apparent resistivity while the cool tones show low apparent resistivity.

977N Schlumberger

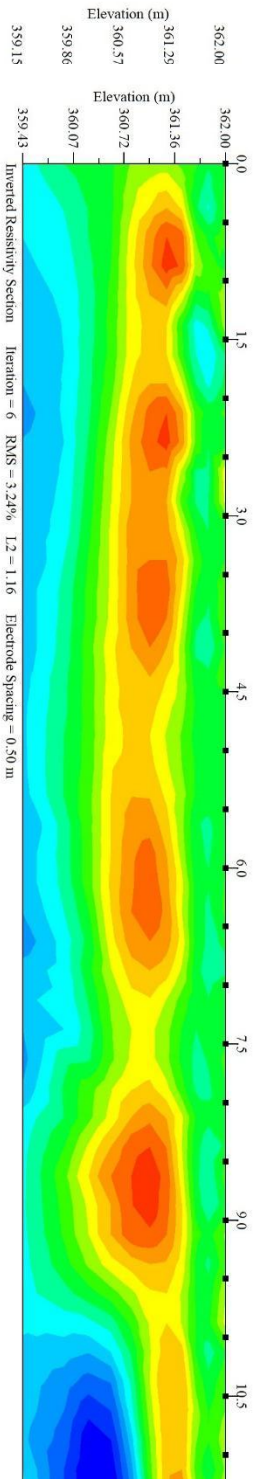
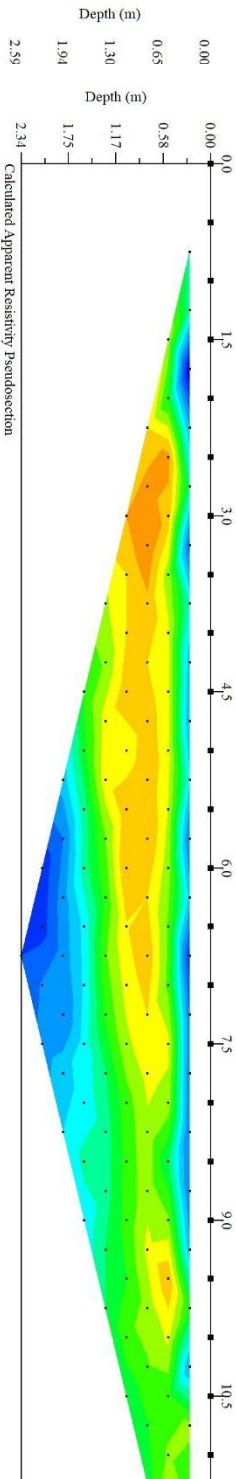
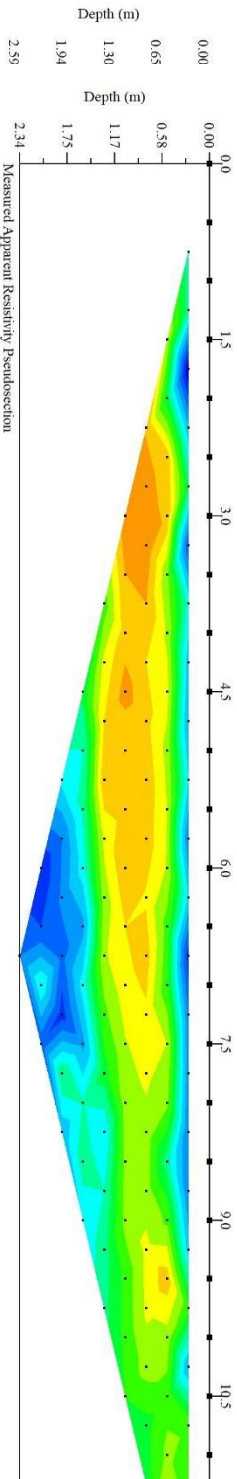


Figure SEQ Figure * ARABIC 10
 (Right): To compare the previous data sets, we decided to create a merger of both the Dipole-dipole and the Schlumberger data. Pictured is this merge. The resultant image is still quite chaotic. The noisy Dipole-dipole data overtook the Schlumberger data, making the image less accurate than the Schlumberger scan on its own. In this case, more data is not the solution

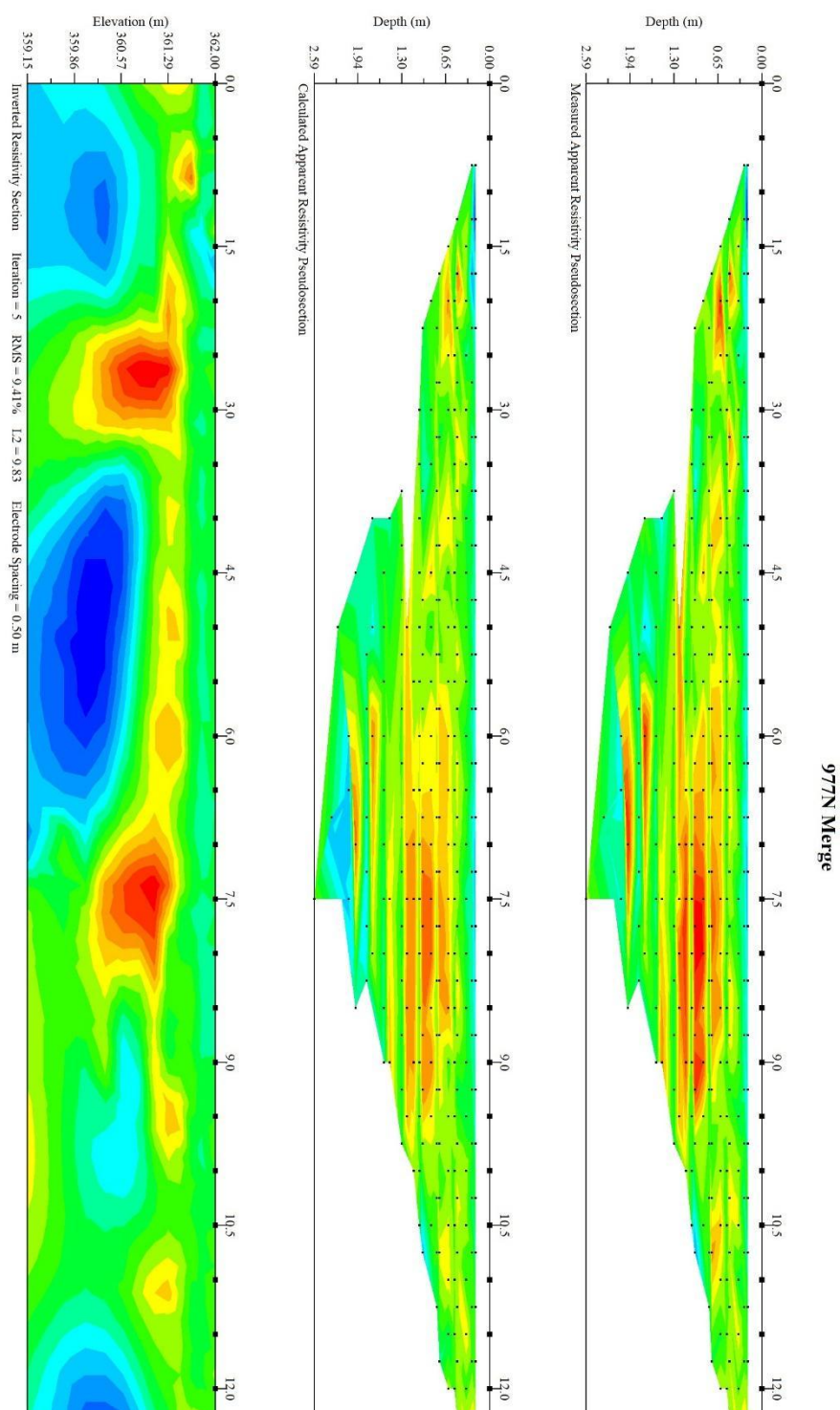


Figure SEQ Figure * ARABIC 11
 (Right): The Dipole-Dipole scans in Taylor Fork resulted in similar, noisy results. Numerous data points required removal like that of the 977N scan. The resultant image is substandard. This is the first of two Taylor Fork Dipole-Dipole scans.

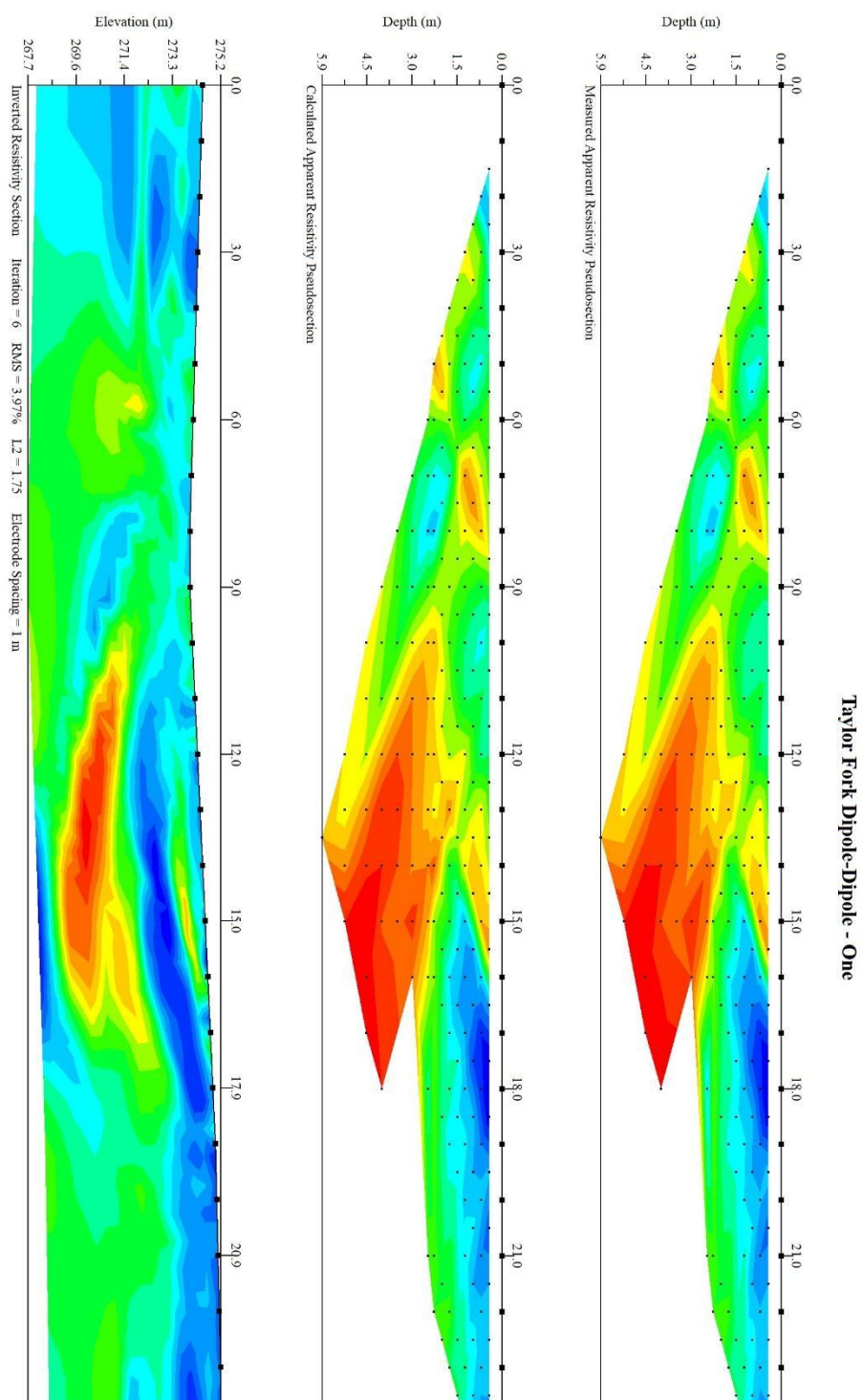


Figure SEQ Figure * ARABIC 12
(Right): This is the second of two Taylor Fork Dipole-Dipole scans. The previous caption applies.

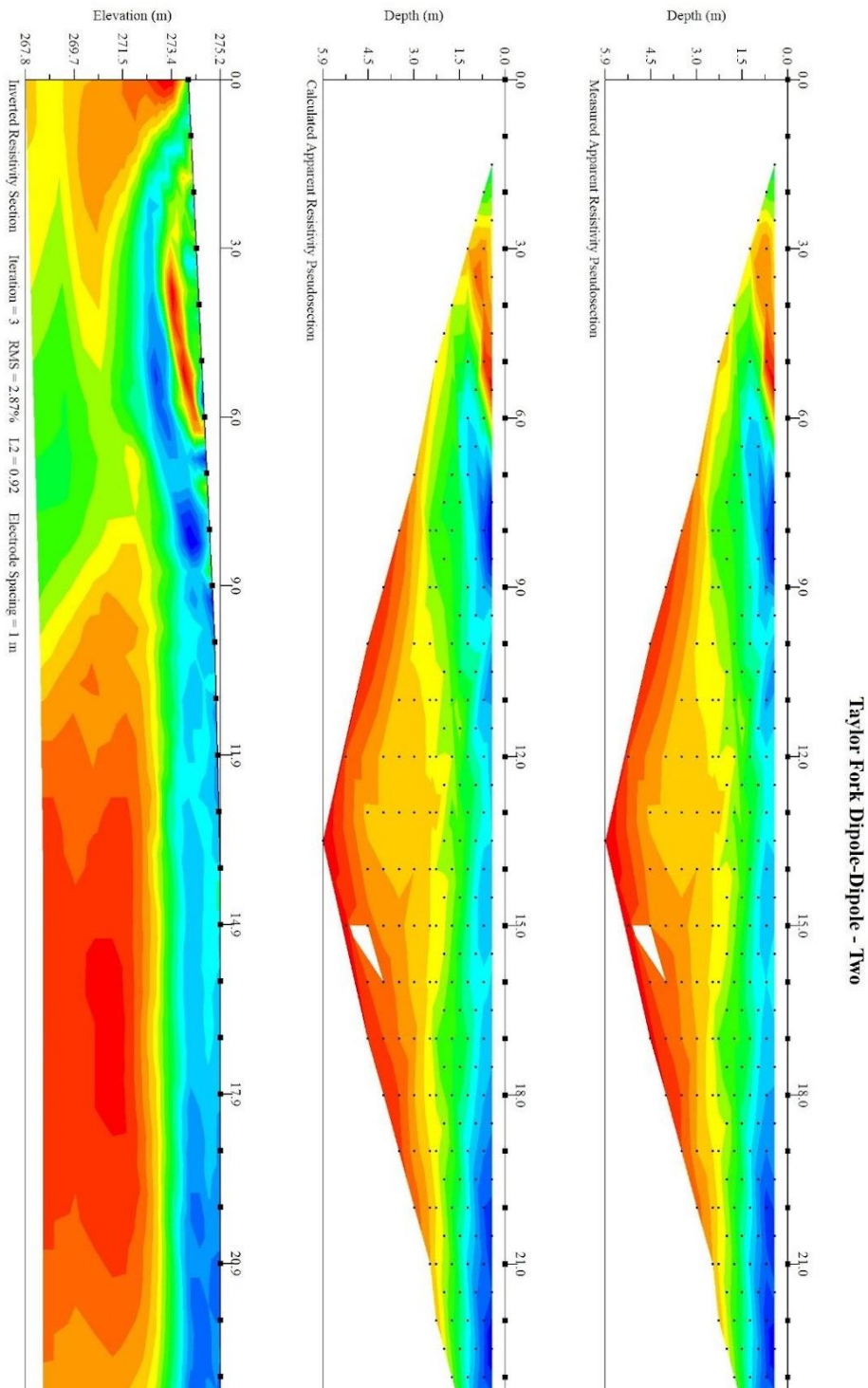


Figure SEQ Figure * ARABIC 13
 (Right): Similarly to the 977N Schlumberger scans, the Taylor Fork Schlumberger scans provided much more accurate data. Little error was found in the raw data, and only a small number of points were removed from the datum. The Schlumberger scan provided a much clearer and ideal image of the Taylor Fork oxbow bend. This is the first of two Taylor Fork Schlumberger scans.

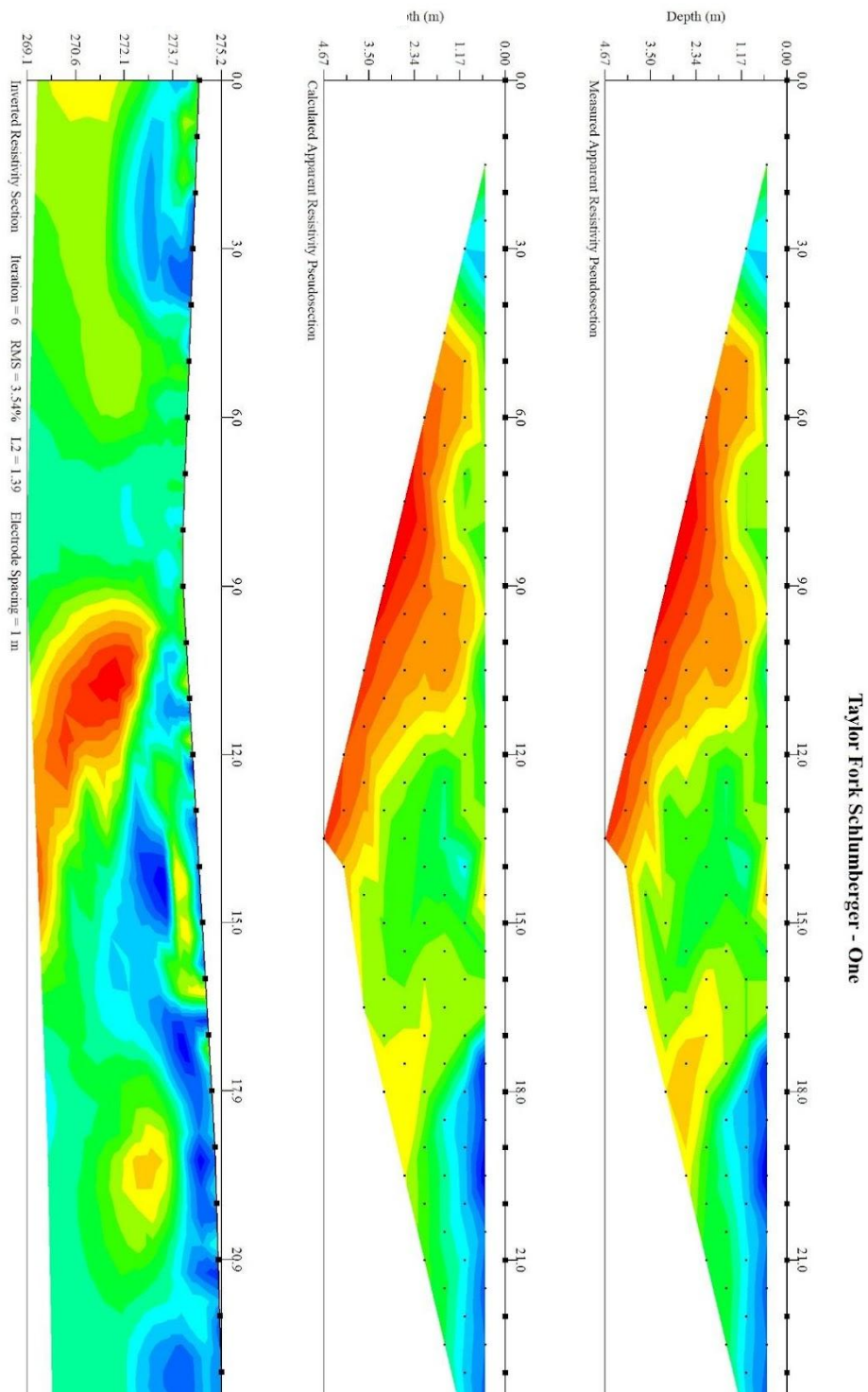


Figure SEQ Figure * ARABIC 14 (Right):
 This is the second of two Taylor Fork Schlumberger scans. The previous caption applies.

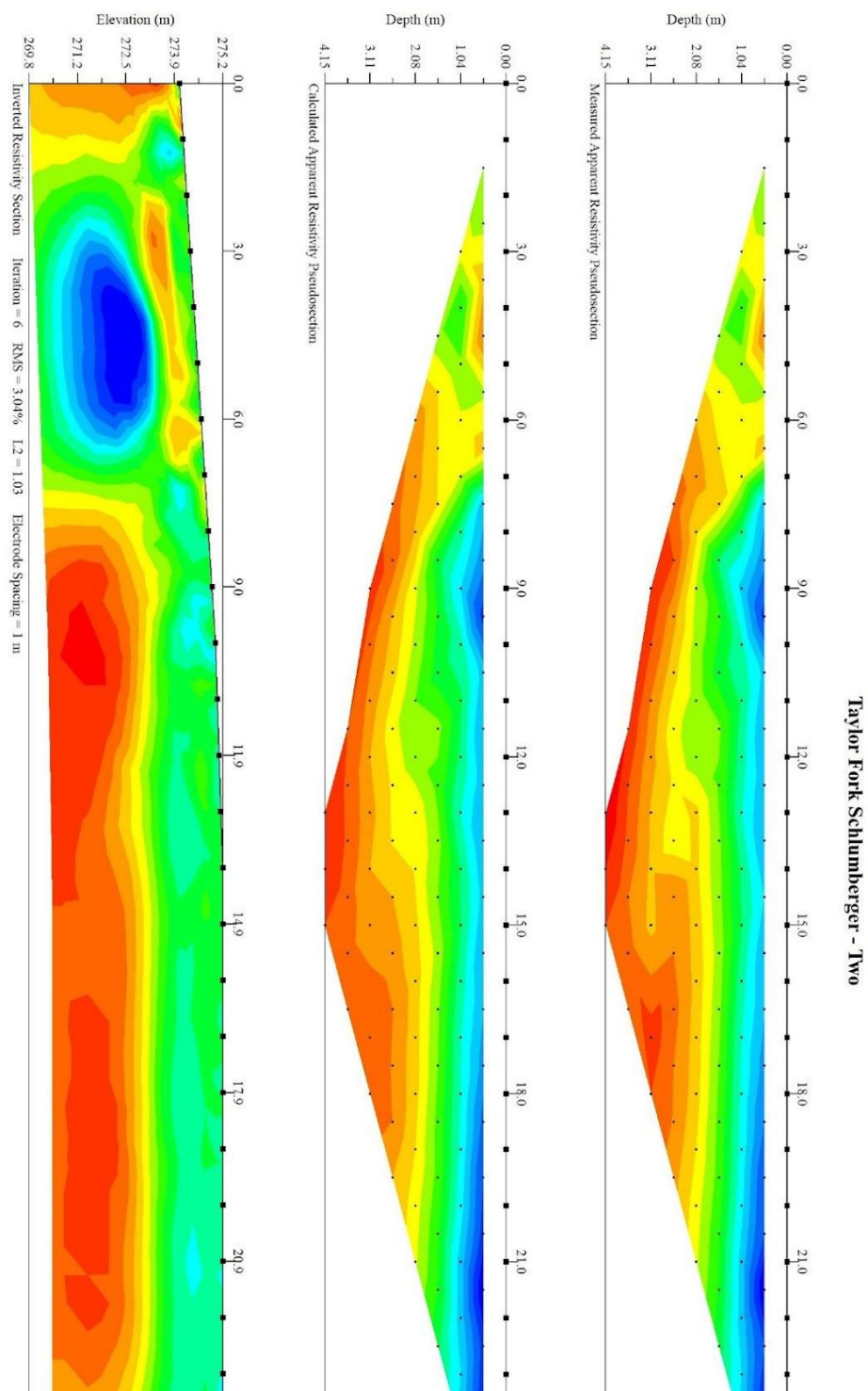


Figure SEQ Figure * ARABIC 15
 (Right): Using both the Schlumberger and Wenner array scans from Taylor Fork, we created a merged data set. The resultant images are pictured. With an incredibly low error and very few points removed, these were the most exemplary pseudosections we processed. This merger provided a clear image of the subsurface in the Taylor Fork Ecological Area. This is the first of two Taylor Fork Wenner-Schlumberger scans.

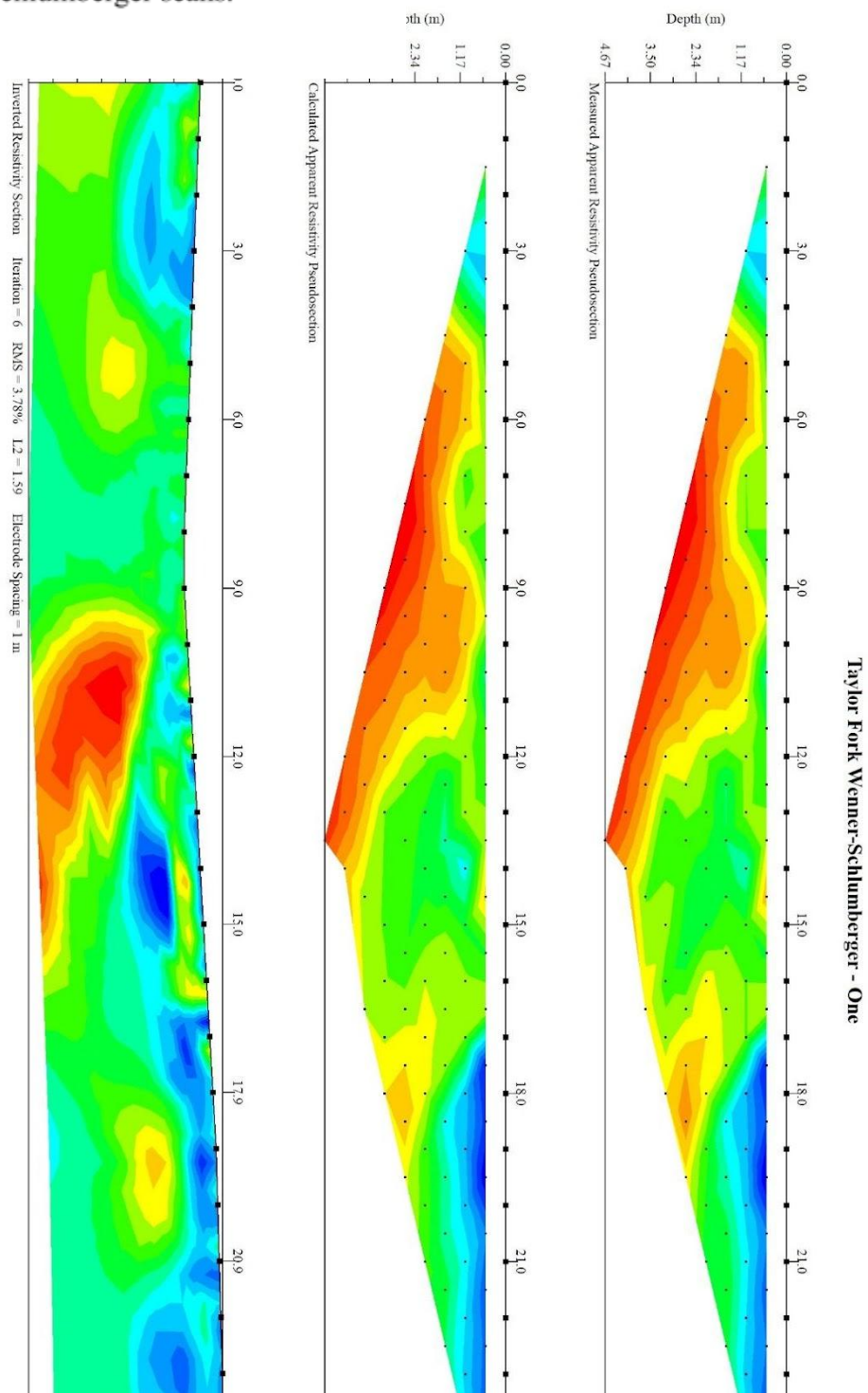
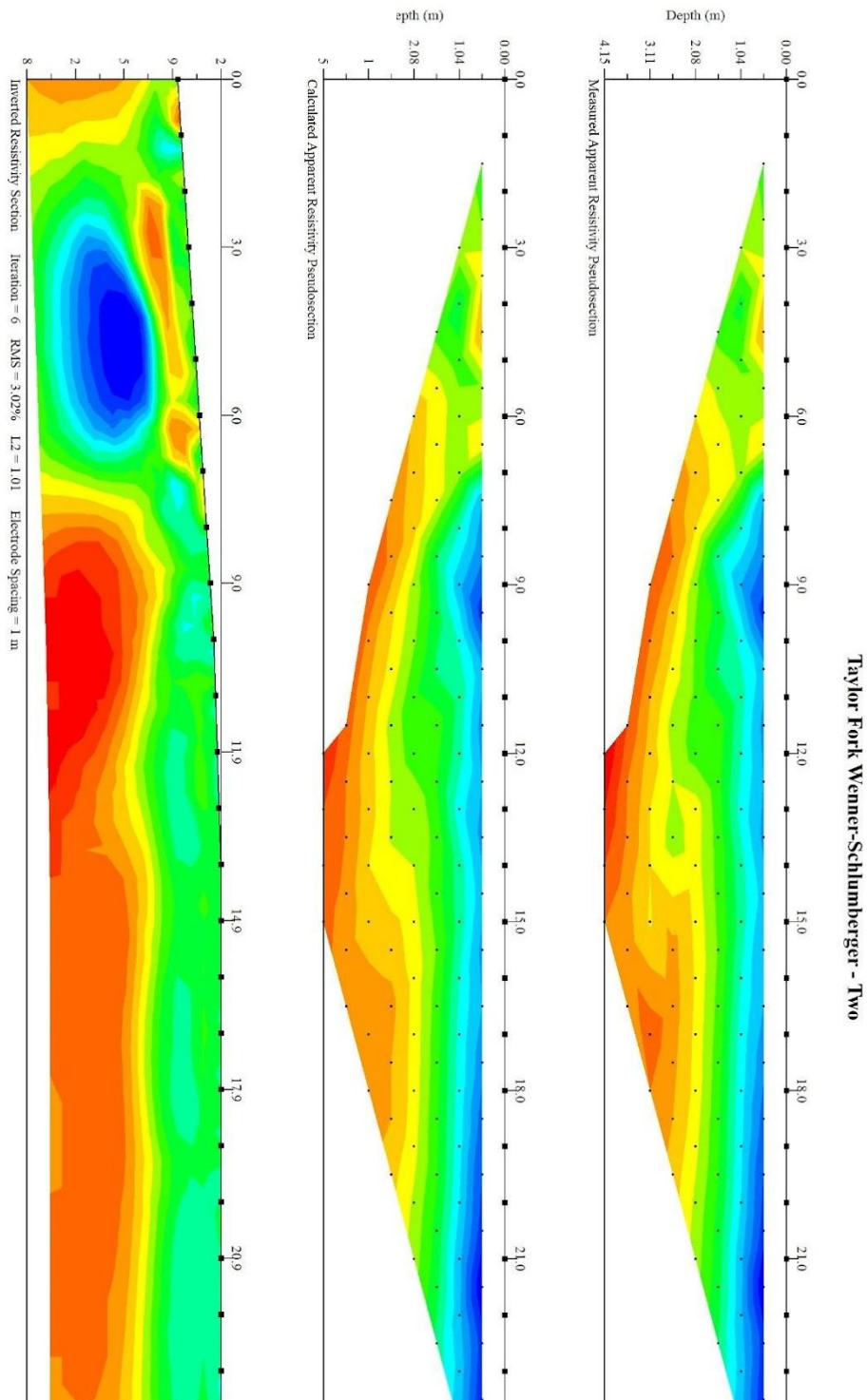


Figure SEQ Figure * ARABIC 16 (Right:
This is the second of two Taylor Fork
Wenner-Schlumberger scans. The previous
caption applies.



Results and Discussion

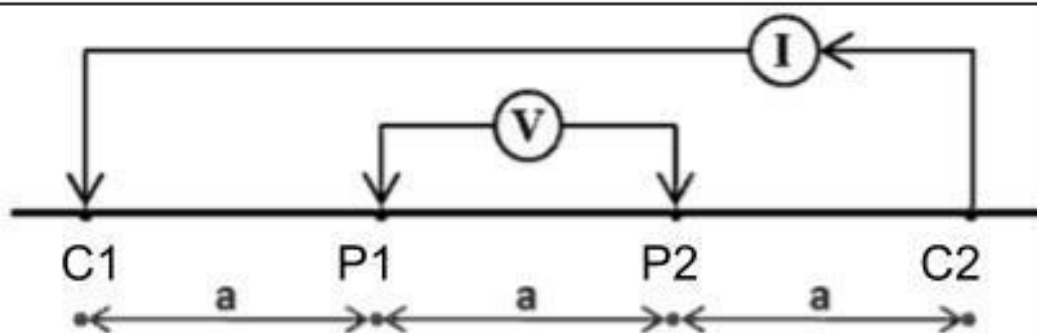
For our research purposes, we compared two commonly used electrode array configurations, Dipole-Dipole and Schlumberger. Both arrays have important differences and uses.

The Wenner array, invented in 1915 by American physicist Frank Wenner, is the simplest of electrode arrays. Four or more electrodes are placed an equal distance from one another (a). The inner two electrodes (P1 and P2) are potential electrodes while the outer two electrodes (C1 and C2) are the current electrodes (*Figure 17*). The Wenner array utilizes the previously mentioned VES method. While still used today, the Wenner array is generally considered outdated and has been replaced by the Schlumberger array (AGIUSA, 2019a).

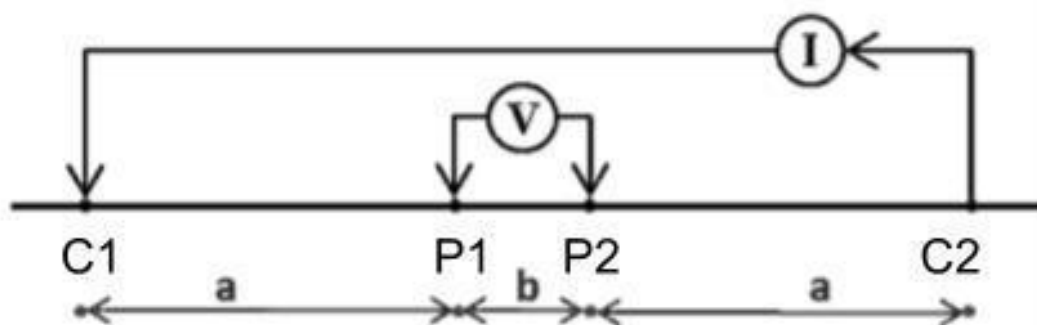
Named after Conrad Schlumberger, the Schlumberger array is one of the most common array configurations. Four or more electrodes are placed in-line with each other, centered around a midpoint. The inner two electrodes (P1 and P2) are potential electrodes while the outer two electrodes (C1 and C2) are the current electrodes (*Figure 17*). Like the Wenner array, this array also utilizes VES. Unlike the Wenner array, the distance between the outer electrodes varies throughout the scan (a), while the inner electrodes maintain the same spacing (b) (AGIUSA, 2019b).

The Dipole-dipole array again consists of four or more electrodes, both potential (P1 and P2) and current (C1 and C2). The word Dipole itself comes from the idea that when two oppositely charged electrodes are in close proximity, a single electric field forms instead of two separate electric poles. Each electrode is placed in a line with equal spacing (a) between them (*Figure 17*). The data is constructed from a series of midpoints

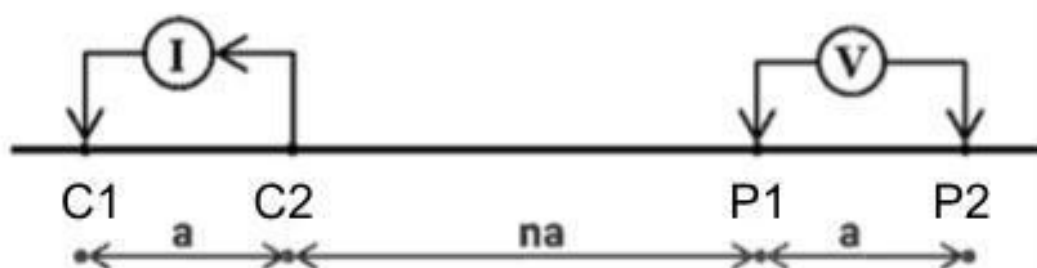
Wenner



Schlumberger



Dipole-Dipole



between the current and potential electrodes. This configuration is capable of producing images with the highest resolution ($= a/2$) but is also the most sensitive to electrical noise (AGIUSA, 2019c).

Conclusion

The results of our study showed that the Schlumberger array configuration was the most effective and accurate reflection of saturated subsurfaces. The resultant pseudosections best reflect previously existing core data (*Figure 7*). The resistivity levels reflect that which we would expect to see from these core samples (Yopp et al., 2021). With lower error levels and considerably less noisy data points, the results recommend this array configuration when working with saturated topsoils.

The Dipole-dipole array configuration proved to yield inferior results, with a substantial amount of noisy data. Much of this data had to be removed during the development of the previously pictured pseudosections. We believe this is due to the high surface conductivity that is characteristic of wetland near-surface soils and other highly saturated soils. It is likely that the currents traveled across the near-surface in addition to traveling below the surface. With this additional current, the resultant data points would prove to be inaccurate, giving a chaotic image of the subsurface.

For future research on the GIWs or other areas of high surface conductivity, we recommend the use of the Schlumberger array. This array will provide a pseudosection that more accurately reflects the subsurface

Appendix One

The following appendix represents the basics of using ERT in the field as well as preliminary data processing techniques. Adapted from former ECU geology major Rebecca Moskal, below lists our processes for this work. Rebecca's work was essential in the beginning stages of this research (Moskal et al., 2021).

Listed is the equipment required for running ERT in the field (*Figure 18*):

1. Power generator
2. SuperSting Power Supply
3. SuperSting R1
4. Switch Box
5. Two sets of electrode cables
6. 28 electrodes (more if available)
7. Several additional connector cables

Additional equipment includes flagging, gloves, mallets, GPS units, and tough boxes (required to protect more delicate equipment).



Below is a simplified step by step procedure of how ERT is set up in the field:

1. Measure desired line in the field site, and mark uniform increments along said line.
2. Hammer electrodes in equivalent distances in line with one another at the previously measured increments. Electrodes must be in a straight line within 10% of said increments. Electrodes must be hammered in straight.
3. Unravel the electrode cables and connect them. Click each cable into the electrodes with electrode 1 being furthest from the SuperSting R1 and electrode 28 being the closest (*Figure 19*).
4. Connect the Switch Box to the SuperSting R1.
5. Connect the power port of the SuperSting R1 to the SuperSting R1 power supplies.
6. Start the generator and connect the generator to the SuperSting Power Supplies.
7. Connect the electrode cable to the Switch Box. It is imperative that this step is taken last as to avoid safety issues involving electricity. Ensure that the field site is clear and flag the area beforehand.



Below in the process of running the ERT and processing the resultant data:

1. Begin with a contact resistivity test. This test ensures that all electrodes have proper connection with one another and are well-seated into the ground surface.
2. Readings for the contact resistivity test should not exceed 1800 Ohms. If this does occur, ensure the electrodes are well seated and that all cables are connected. For values that exceed 1000 Ohms it is recommended that the field technician saturate the ground immediately around the electrode with water.
3. Once a satisfactory contact resistivity test occurs, create a new data file and select a command file. The command file determines the type of array configuration that is to be used. Additional information will also need to be entered including measurements of the line, spacing between electrodes, and number of electrodes.
4. After this setup process, continue to the Switch Box menu. Proceed through each menu, keeping the default settings unless otherwise desired.
5. Begin the test. During this time the line should not be approached or touched for safety reasons. For our purposes, tests range from 17 to 60 minutes, depending on the array configuration used. The resistivity data will populate on the screen in real time. Ensure that these numbers are consistent with expected values.
6. Final data are processed using AGI EarthImager 2D. After connecting the Brain Box to the computer, download the new files.
7. Run an inversion in the software and view the misfit cross plot. A terrain file may be added if desired. Up to 20% of noisy data can be removed without compromising the work. Final models should ideally have an RMS error below 5%. Noisy data sets can sit below 10%. Final images can be saved as .jpeg files.

References

- AGIUSA, 2019a, Wenner Array: Electrical Resistivity Methods, Part 1: AGIUSA,
https://www.agiusa.com/wenner-array?utm_campaign=Non-Hosted+AGI+Blog&utm_source=AGI+Blog+Best+Array&utm_medium=link&utm_content=Link+from+Best+Array+to+Wenner. (accessed November 2022).
- AGIUSA, 2019b, Schlumberger Array: Electrical Resistivity Methods, Part 2: AGIUSA,
https://www.agiusa.com/schlumberger-array?utm_campaign=Non-Hosted+AGI+Blog&utm_source=AGI+Blog+Best+Array&utm_medium=link&utm_content=Link+from+Best+Array+to+Schlum. (accessed November 2022).
- AGIUSA, 2019c, Dipole-Dipole Array: Electrical Resistivity Methods, Part 3: AGIUSA,
https://www.agiusa.com/dipole-dipole%E2%80%8B-%E2%80%8Barray%E2%80%8B?utm_campaign=Non-Hosted+AGI+Blog&utm_source=AGI+Blog+Best+Array&utm_medium=link&utm_content=Link+from+Best+Array+to+DipDip. (accessed November 2022).
- AGIUSA, 2022a, Agi Earthimager™ 2d: AGIUSA, <https://www.agiusa.com/agi-earthimager-2d>. (accessed November 2022).
- AGIUSA, 2022b, How Do I Perform a Receiver Test for My Supersting™ R1 to R8 WIFI (Also All Pre WIFI R8 Models)? : AGI Help Desk,
<https://helpdesk.agiusa.com/supersting-wifi/supersting-troubleshooting/how-do-i-perform-a-receiver-test-for-my-supersting>. (accessed November 2022).
- AGIUSA, 2022c, Supersting™ R8 Adapter Box: AGIUSA,
<https://www.agiusa.com/supersting%E2%84%A2-r8-adapter-box>. (accessed November 2022).

AGIUSA, 2022d, Supersting™ Wi-Fi: AGIUSA, <https://www.agiusa.com/supersting-wifi>.
(accessed November 2022).

Beall, B.B., 2020, Wetland Words and What They Mean: Soil-Related Words: New York State Wetlands Forum. <http://www.wetlandsforum.org/fagsoils.htm> (accessed October 2022).

Climate Data, 2022, Climate Kentucky: Climate Data.
<https://en.climate-data.org/north-america/united-states-of-america/kentucky-988/>.
(accessed November 2022).

Dixon, M. J. R., Loh, J., Davidson, N. C., Beltrame, C., Freeman, R., & Walpole, M., 2016, Tracking global change in ecosystem area: The Wetland Extent Trends index: Biological Conservation, v. 193, p. 27-35. <https://doi.org/10.1016/j.biocon.2015.10.023> (accessed November 2022).

Everest Geophysics, 2019, Vertical Electrical Soundings: Everest Geophysics,
<https://everestgeophysics.com/methods/electric/vertical-electrical-soundings/>. (accessed November 2022).

Garofalo, F., 2014, Physically constrained joint inversion of seismic and electrical data for near-surface application. <https://doi.org/10.1190/geo2014-0313.1> (accessed November 2022).

Golden, H.E., Creed, I.F., Ali, G., Basu, N.B., Neff, B.P., Rains, M.C., McLaughlin, D.L., Alexander, L.C., Ameli, A.A., Christensen, J.R., Evenson, G.R., Jones, C.N., Lane, C.R., and Lang, M., 2017, Integrating geographically isolated wetlands into land management decisions: Frontiers in Ecology and the Environment, v. 15, no. 6, p. 319-327.
<https://doi.org/10.1002/fee.1504>. (accessed June 2022).

Koch, B., 2022, What Are the Different Types of Wetland Soils?: All Things Nature.

<https://www.allthingsnature.org/what-are-the-different-types-of-wetland-soils.htm>

(accessed November 2022).

Kunkel, K.E., 2022, State Climate Summaries 2022: NOAA National Centers for Environmental Information, <https://statesummaries.ncics.org/chapter/ky/>. (accessed October 2022)

Moreira, C.A., Rosolen, V., Furlan, L.M., Bovi, R.C., and Masquelin, H, 2021, Hydraulic conductivity and geophysics (ERT) to assess the aquifer recharge capacity of an inland wetland in the brazilian savanna: Environmental Challenges, v. 5, p. 100274.

<https://doi.org/10.1016/j.envc.2021.100274>. (accessed June 2022).

Moskal, R., White, J.C., and Malzone, J.M., 2020. Electrical resistivity tomography (ERT) applied to an investigation of ridgetop wetland hydrogeology in the Daniel Boone National Forest, Rowan County, Kentucky. Geological Society of America Abstracts with Programs, v. 52, n. 6, doi: 10.1130/abs/2020AM-356472.

National Research Council, 1995, Wetlands: Characteristics and Boundaries: The National Academies Press. <https://doi.org/10.17226/4766>. (accessed November 2022).

Okopokhi, I.S. and White, J.C., 2019. Detection of sinkholes and other karst features using electrical resistivity tomography in Richmond, Kentucky. Geological Society of America Abstracts with Programs, v. 51, n. 2, doi: 1130/abs/2019SC-326286.

Reed, P., 2022, What Is a Resistivity Meter?: All the Science, <https://www.allthescience.org/what-is-a-resistivity-meter.htm>. (accessed November 2022).

Rosa, F.T., Moreira, C.A., Rosolen, V., Casagrande, M., Bovi, R.C., Furlan, L.M., and dos Santos, S.F., 2022, Detection of aquifer recharge zones in isolated wetlands: Comparative

analysis among electrical resistivity tomography arrays: *Pure and Applied Geophysics*, v. 179, no. 4, p. 1275–1294. <https://doi.org/10.1007/s00024-022-02987-0>. (accessed June 2022).

Tiner, R.W., 2003, Geographically isolated wetlands of the United States: *Wetlands*, v. 23, p. 494–516, [https://doi.org/10.1672/0277-5212\(2003\)023\[0494:GIWOTU\]2.0.CO;2](https://doi.org/10.1672/0277-5212(2003)023[0494:GIWOTU]2.0.CO;2) (accessed October 2022).

Tiner, R.W., Bergquist H. C., DeAlessio G. P., and Starr M. J., 2002, Geographically Isolated Wetlands: A Preliminary Assessment of their Characteristics and Status in Selected Areas of the United States: U.S. Department of the Interior, Fish and Wildlife Service, Northeast Region, Hadley, MA.
<https://www.fws.gov/wetlands/Documents%5CGeographically-Isolated-Wetlands-A-Preliminary-Assessment-of-their-Characteristics-and-Status-in-Selected-Areas-of-the-United-States-NI.pdf> (accessed October 2022).

Yopp, B.M., Moskal, R., Malzone, J.M., and White, J.C., 2021. The use of Electrical Resistivity Tomography for delineating ridgetop wetland hydrogeology in the Daniel Boone National Forest in eastern Kentucky. Kentucky Water Resources Research Institute, Annual Symposium, Lexington, KY.